

# Modeling Pollutant Buildup and Washoff Parameters for SWMM Based on Land Use in a Semiarid Urban Watershed

Min-Cheng Tu · Patricia Smith

Received: 1 December 2017 / Accepted: 6 March 2018  
© Springer International Publishing AG, part of Springer Nature 2018

**Abstract** SWMM (Storm Water Management Model) has been widely used in urban water resources management. Despite its popularity, no commonly accepted pollutant buildup and washoff parameters are available for urban areas in semi-arid or arid climate, which covers 30% of global land area and is sustaining fast growth. This study provides a method to determine these parameters using inverse modeling and apply it in a semi-arid Texan urban watershed. Because GIS land use data is not available for early 1980s, it was determined from aerial photography from 1984 to 2006, and GIS land use data from 2006. Calibration using Shuffled Complex Evolution – University of Arizona (SCEUA) was used for hydraulic parameters followed by pollutant parameters. Confidence intervals of pollutant parameters were calculated by GLD (Generalized Lambda Distribution). Buildup parameters are clustered in narrow numerical ranges, indicating that spatially uniform factors are responsible for pollutant buildup. Washoff parameters do not cluster and are distributed more evenly, indicating strong influence of local factors such as

topography. The results also imply that the commonly used parameter values need major revision.

**Keywords** Buildup · Inverse modeling · SCEUA · Semiarid · SWMM · Washoff

## 1 Introduction

Different types of land use deliver different pollutants to urban streams from the different kinds of human activities they carry. In the USA, the National Urban Runoff Program (NURP) is one of the first programs to determine such differences using field measurements (Urbonas and Stahre 1993; United States Environmental Protection Agency [U.S. EPA] 1983). The NURP concluded that no statistically significant differences exist in pollutant-providing capabilities between different land uses in the USA. NURP's conclusions were generalized for the entire USA (i.e., ignoring regional difference), but other smaller scale studies worldwide based on either event mean concentrations (EMC) (Park et al. 2009) or linear buildup rates from urban surfaces (Wicke et al. 2012; Wang and Li 2009; Huber and Dickinson 1988) arrived at different conclusions. For those small-scale studies, different land uses did generate runoff containing different pollutant concentrations.

The first version of SWMM (Storm Water Management Model) was introduced by the U.S. EPA in 1971 (Rossman 2010) and was extremely popular in urban water resources management since then. SWMM is capable of simulating pollutant delivery by using

---

M.-C. Tu (✉)  
Department of Civil and Environmental Engineering, Villanova University, Villanova, PA 19085, USA  
e-mail: min-cheng.tu@villanova.edu

M.-C. Tu  
Villanova Urban Stormwater Partnership (VUSP), Villanova University, Villanova, PA 19085, USA

P. Smith  
Department of Biological and Agricultural Engineering, Texas A&M University, College Station, TX 77843, USA

buildup and washoff equations. Correctly parameterizing the equations for different land use is important for utilizing the full potential of SWMM.

Three buildup equations (power, exponential, and saturation) and three washoff equations (exponential, rating curve, and event mean concentration) are provided in SWMM (Rossmann 2010). Parameters of exponential buildup and exponential washoff equations are frequently reported in literature as Table 1 shows. Therefore, this study considered only parameters of the exponential buildup (Eq. 1) and washoff (Eq. 2) equations, so the results are comparable. The equations are as follows:

$$\text{Buildup} = C_1 \cdot (1 - \exp(-C_2 \cdot t)) \quad (1)$$

$$\text{Washoff} = C_3 \cdot \text{Runoff}^{C_4} \cdot \text{Buildup}' \quad (2)$$

In Eq. 1, the buildup term on the left-hand side is the pollutant buildup in mass per unit area or unit curb length, and  $t$  on the right-hand side is the number of preceding dry weather days. In Eq. 2, the washoff term on the left-hand side is the washoff load in the unit of mass per hour, the runoff term on the right-hand side is runoff rate per unit area (inches/h or mm/h), and  $\text{Buildup}'$  is the pollutant buildup in units of total mass.  $C_1$  is the maximum buildup possible (mass per unit area or unit curb length),  $C_2$  is the buildup rate constant controlling the speed of pollutant buildup (1/days),  $C_3$  is the washoff coefficient, and  $C_4$  is the washoff exponent.

In the literature, researchers have resorted to either computer modeling or small-scale field measurements in order to determine parameters  $C_1$ – $C_4$ . Some of these efforts have been summarized in Table 1.

In Table 1, the buildup and washoff parameters vary significantly from one location to another, as urban runoff pollution is influenced (Tsihrintzis and Hamid 1997) by both local (e.g., traffic volume, land use, geographic/geologic characteristics, maintenance practice, drainage system configuration) and climate factors (e.g., rainfall pattern, rainfall volume, rainfall intensity, antecedent dry days). A more versatile and universal approach is needed to derive the parameters from any location of interest. In addition, two points are also derived from Table 1:

1. Locations where experimental data was collected from Table 1 are all located in the humid climate.

No similar study has been performed for locations of semiarid and/or arid climates, in which the rainfall pattern is drastically different from that in the humid climate (Hernandez et al. 2000). Semiarid and arid regions represent approximately 30% global land area, and they are among the most fast-growing regions worldwide (Scanlon et al. 2006). Since climate is a major factor controlling urban runoff pollution, it is imperative to have a study providing baseline values for pollutant parameters from semiarid and/or arid regions.

2. The results in Table 1 are limited in land use with only one study (Chow et al. 2012) exploring the parameters for commercial and industrial land uses.

Therefore, the purpose of this study is two-fold:

1. This study will present a methodology to derive the pollutant buildup and washoff parameters, so users worldwide can derive these parameters for their own area of interest.
2. Applying the methodology, this study will provide baseline values for pollutant parameters of multiple land uses in a semiarid urban region.

## 2 Research Area

The subwatershed of Walnut Creek from the City of Austin was used in this analysis. The Walnut Creek Watershed at Webberville Rd. lies in the eastern part of the city with a total area of 13,287 ha. The elevation change throughout the landscape is gentle, ranging from 285 m in the north to 132 m in the south, which gives a mean slope of approximately 1%. Most soil types in the watershed are clayey as delineated in the Web Soil Survey (Natural Resources Conservation Services [NRCS] 2017), so storms can create significant runoff due to the low hydraulic infiltration rate of clay.

Austin has a bimodal distribution of precipitation, with annual precipitation around 84 cm (National Climatic Data Center [NCDC] 2017). Thunderstorms triggered by the interaction between moist air from the Gulf of Mexico and the dry air from the Rocky Mountains are the main source of precipitation. Based on the definition of UNESCO (United Nations Educational, Scientific, and Cultural Organization), Austin is in the region of semiarid climate because it has a ratio of mean annual

**Table 1** Parameters for exponential buildup and washoff equations in SWMM from literature studies

Study	Location	Land use	Pollutant	$C_1$	$C_2$	$C_3$	$C_4$
Chow et al. 2012	Malaysia	Residential	TSS	0.003 (kg/m curb)	0.8	0.2	1.4
			TP	0.003 (kg/m curb)	0.05	0.41	1.46
		Commercial	TSS	0.015 (kg/m curb)	0.8	1.4	0.9
			TP	0.0005 (kg/m curb)	0.1	0.4	1
		Industrial	TSS	0.013 (kg/m curb)	0.7	3	0.6
			TP	0.0003 (kg/m curb)	0.16	0.8	1.08
Hossain et al. 2012	Australia	Residential impervious	TSS	–	–	0.03	0.21
			TN	–	–	0.004–0.005	0.65–0.8
			TP	–	–	0.0003–0.0004	0.75–0.9
		Pervious	TSS	–	–	0.05–0.055	0.21
			TN	–	–	0.0065–0.008	0.65–0.8
			TP	–	–	0.0005–0.0007	0.75–0.9
Wicke et al. 2012	New Zealand	Urban	TSS (concrete)	27.6 (kg/ha)	0.2	0.24	1
			TSS (asphalt)	13.4 (kg/ha)	0.23	0.27	1
Hossain et al. 2010	Australia	Urban	TSS (road)	53 (kg/ha)	0.222	0.0029–0.0135	0.608–0.986
				27.5 (kg/ha)	0.21	0.0015–0.0059	0.945–1.27
				26 (kg/ha)	0.382	0.0062–0.011	0.753–0.914
			TSS (roof)	8.5 (kg/ha)	0.188	0.051–0.202	0.363–0.603
Hood et al. 2007	Estonia	Urban	TSS <sup>a</sup>	25 (kg/ha)	1	4.9	1.57
			TN <sup>a</sup>	0.15 (kg/ha)	0.0015	250	1
			TP <sup>a</sup>	0.25 (kg/ha)	0.0025	500	2.35
Temprano et al. 2006	Spain	Residential	TSS	0.046 (kg/m curb)	0.3	1.811	1
				17.5 (kg/ha)	0.3	1.811	1
			COD	0.0027 (kg/m curb)	0.3	3.937	1
				1.02 (kg/ha)	0.3	3.937	1
			TN	0.0001 (kg/m curb)	0.3	8.661	1
Barco et al. 2004	Italy	Residential	TSS	18 (kg/ha)	0.3	0.13	1.2
				impervious)			

<sup>a</sup> Unit not given. Presumed to be kg/ha because of its numerical range

precipitation to potential evapotranspiration (PET) between 0.2 and 0.5 (Scanlon et al. 2006).

### 3 Methodology

#### 3.1 Summary

This study will utilize inverse modeling to derive the buildup and washoff parameters for total suspended solid (TSS), total nitrogen (TN), and total phosphorus (TP) in a watershed in Austin, Texas. Inverse modeling

backtracks parameters from the measured data (Ines and Droogers 2002). Utilizing observations at the outlet of a watershed, inverse modeling has been successfully used by studies to derive pollutant parameters (Hossain et al. 2012). Because the distributions of parameters from multiple calibration runs were found to be mostly bimodal from this study, they will be fit by GLD (Generalized Lambda Distribution), so confidence intervals can be calculated.

The USGS (United States Geological Survey) stream water quality data (USGS 2017a) is used to represent overland runoff water quality. However, the use of Best

Management Practices (BMP), such as stormwater retention ponds, has become prevalent in recent decades (Urbonas and Stahre 1993). Since 1990, cities in the USA have been required to install BMPs as part of their stormwater management programs under the direction of NPDES—National Pollutant Discharge Elimination System. As of 2012, the City of Austin, TX, had over 7000 B.P. registered in the greater Austin area, up from just over 100 in the early 1980s (City of Austin 2017). BMPs mitigate stormwater quality, so the link between stream water quality and overland runoff water quality is broken. Since BMPs interfere with the determination of native pollutant buildup and washoff parameters, so a watershed free of BMPs is desirable in inverse modeling of parameters. So, only data from early 1980s was used in this study.

Due to rapid development in the past decades, land use from the early 1980s in Austin, TX, needs to be determined, so the SWMM model can be correctly parameterized. An approach utilizing both aerial photographs in 1984 and 2006 as well as expert judgment was applied to determine the land use in 1984.

### 3.2 Data Availability

The sources of the data used in this study are summarized in Table 2. The only data source that is not readily available in Table 2 is land use data, which will be discussed below.

### 3.3 Land Use Determination

Land use from 1984 required special attention because no detailed land use data was available for Austin in the

early 1980s. Land use in 1984 was derived from three sources: aerial photography from 2006, aerial photography from 1984, and GIS land use data from 2006 (City of Austin 2017). Figure 1 contains a flow chart for illustrating the process for land use determination. The determination was done for individual city blocks.

First, aerial photographs from 1984 and 2006 were visually compared for each city block. The differences were categorized into two types: (1) Undeveloped land in 1984 becomes developed in 2006 (i.e., urban expansion), and (2) rezoning or rebuilding of lots. The first type, which is the most common, was easier to handle by simply converting the new urban area (2006) back to undeveloped land use (1984). For the second type of correction, the unknown land use in 1984 was determined by comparing the block of question with other parts of the 1984 aerial image where land uses had been determined. All edits were done on the GIS land use data from 2006 to generate the land use of 1984. The 1984 land use distribution of the Walnut Creek Watershed at Webberville Rd. is shown in Fig. 2.

### 3.4 Stormwater Management Model (SWMM)

SWMM simulates the quantity and quality of surface water by separating the water cycle into the land surface compartment, the atmosphere compartment, the groundwater compartment, and the transport compartment (Rossman 2010). The atmosphere compartment simulates the distribution of rainfall. The watershed is divided into a number of subcatchments in the land surface compartment. Water infiltration is simulated by the land surface compartment by one of the three methods: (1) Horton's equation, (2) Green-Ampt equation, or (3)

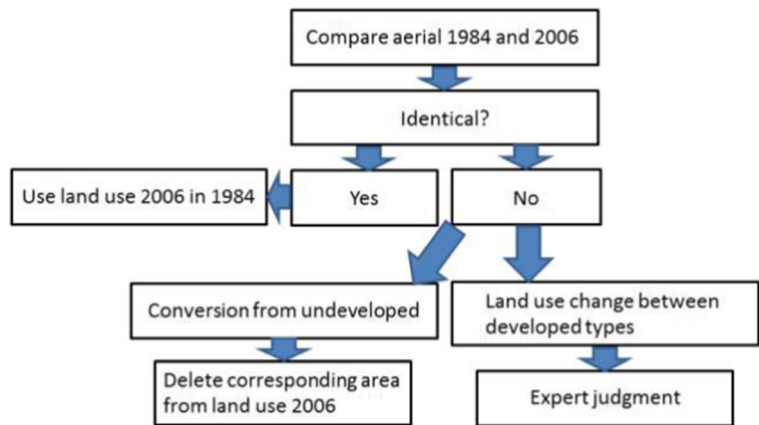
**Table 2** Data used in the current study

Data	Data date	Format	Source
Elevation	n/a	10-m DEM raster	(USGS 2017b)
Imperviousness	2001	30-m raster	(MRLC <sup>a</sup> 2017)
Land use	1984	GIS shape file	Derived in this study
Stormwater sewer network	2012	GIS database	(City of Austin 2012) <sup>b</sup>
River network	n/a	GIS shape file	(USGS 2017b)
Channel cross section	1982–1985	Field survey	(USGS 2017a)
Precipitation	1982–1985	Hourly mean	(NCDC 2017)
Runoff	1982–1985	Daily mean	(USGS 2017a)

<sup>a</sup> Multi-Resolution Land Characteristics Consortium

<sup>b</sup> Data acquired from City of Austin by personal communication

**Fig. 1** Flow chart of land use determination used in this study



Curve Number equation. Runoff is considered the excess of rainfall after evaporation (calculated by temperature or user input values) and infiltration are accounted for.

The groundwater compartment separates soil into the unsaturated zone and the saturated zone (i.e., groundwater aquifer). The hydrologic connection between the unsaturated and saturated zones is calculated using Darcy’s Law (Huber and Dickinson 1988). If the

elevation of saturated zone (i.e., water table) is higher than that of the surface water, the groundwater aquifer can connect with the surface water to provide baseflow, and vice versa.

The transport compartment simulates water flow in all conveyance elements (channels, pipes, pumps, regulators, etc.) and storage/treatment devices by link and node objects, which are connected to subcatchments in the land surface compartment and baseflow in the

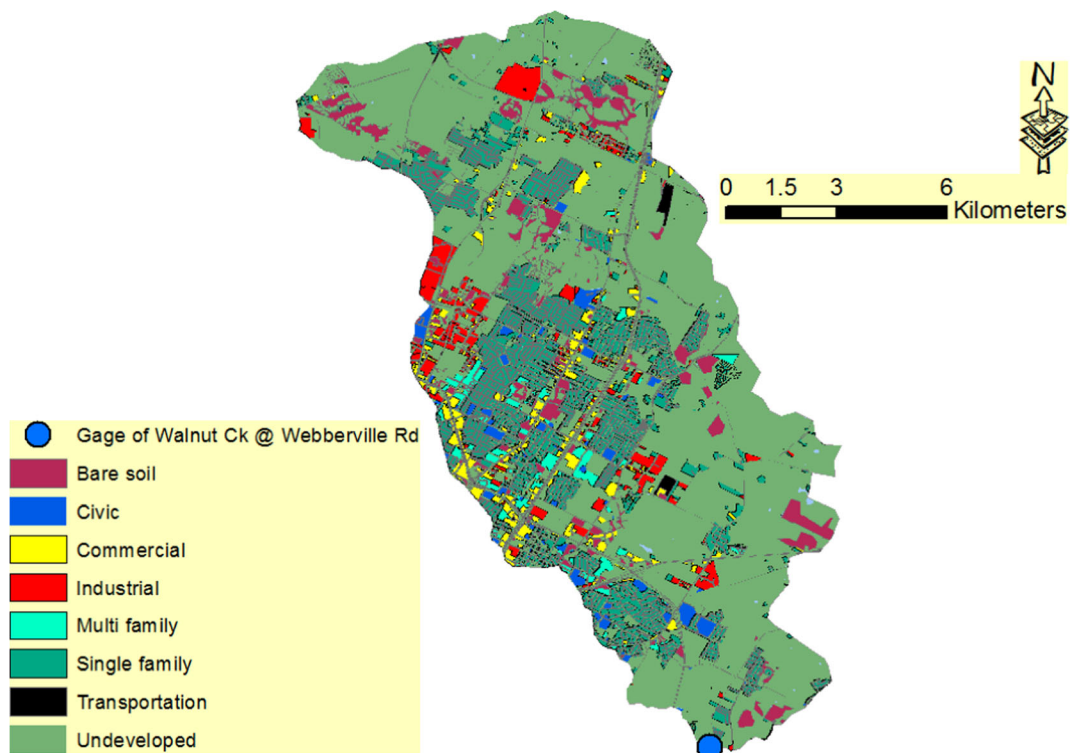


**Fig. 2** Land use distribution in the Walnut Creek Watershed at Webberville Road in 1984 derived from aerial photography and 2006 land use

groundwater compartment. SWMM provides three options in simulating flow routing: steady flow, kinematic wave, and dynamic wave routing. Steady flow routing is “no routing,” which transfers the upstream hydrographs to downstream without change. Kinematic routing considers only the effect of conduit friction (calculated by Manning’s equation under unpressurized conditions) in St. Venant equations and omits inertial and pressure forces and backwater effects. Dynamic routing considers all components in the St. Venant equations but needs small computational time steps.

### 3.5 Model Construction

All stormwater sewers installed after 1984 were deleted on the 2012 stormwater sewer network based on the data attributes in the GIS database. The remaining manholes, inlets, and junction points were used to create subcatchments with the minimum area threshold of 2 ha. This procedure generated 168 subcatchments for use in SWMM simulation. To accelerate the modeling process (set-up and run time), stormwater sewers were simplified (Leitao et al. 2010; Fischer et al. 2009) to keep only the skeleton sewer network.

Hourly precipitation data from five NCDC (National Climatic Data Center) weather stations (Granger Dam, Georgetown Lake, Spicewood, Red Rock, and Camp Mabry) was used (NCDC 2017). Precipitation at each subcatchment is calculated by inverse distance weighting (IDW) from the four weather stations with a power parameter of two (Ruelland et al. 2008).

Only direct runoff is simulated in this study, so parameters in the SWMM groundwater compartment do not need to be calibrated as they are not used. The observation data from the gage of Walnut Ck @ Webberville Rd. (USGS site number 08158600) was processed by baseflow separation by the digital filter method (Lim et al. 2005) using settings for porous aquifers, so the simulated and observed data is comparable.

The initial values and allowed numerical ranges of parameters in hydraulic parameter calibration follow recommendations from the SWMM user’s manual. As for the pollutant parameters (i.e., buildup and washoff parameters) of TSS, TN, and TP, the initial values were chosen as mean values from Table 1 and the ratios of maximum/mean and mean/minimum are based on the same ratios of event mean concentrations (EMC) in the NURP report (U.S. EPA 1983).

Runoff data from 36 events with direct runoff larger than twice the average daily direct runoff were selected between February 1983 and February 1985 for model calibration and validation. These 36 events were further split into two groups, calibration and validation, respectively, with similar distributions in the magnitude and duration of events in both groups.

The model was calibrated using the Shuffled Complex Evolution–University of Arizona (SCEUA) module in the model-independent Parameter Estimation and Uncertainty Analysis (PEST) (Doherty 2010). SCEUA starts with an initial random population of parameter sets. The population is divided into a number of complexes, and each complex is evolved separately. The population with the lowest value for the objective function is dropped. Sum of square of the residuals was used as the objective function. This completes a loop and the algorithm enters the next loop by dividing the population into complexes again, as described above. The detailed algorithm is described by Duan et al. (1993).

Accuracy of calibration and validation was assessed using Nash–Sutcliffe Efficiency (NSE) (Eq. 3). NSE ranges from  $-\infty$  to 1, where NSE of 1 indicates a perfect fit between measured and predicted values.  $Q_o^t$  represents observed flow rate at time  $t$ ,  $Q_m^t$  represents modeled flow rate at time  $t$ , and  $\bar{Q}_o$  represents the average of observed flow rates. Following calibration, the hydraulic model had a NSE of 0.76 and the validation group had a NSE of 0.70. The calibrated model showed negligible runoff and routing error in SWMM, at  $-0.124$  and  $0.182\%$ , respectively.

$$NSE = 1 - \frac{\sum_{t=1}^T (Q_o^t - Q_m^t)^2}{\sum_{t=1}^T (Q_o^t - \bar{Q}_o)^2} \quad (3)$$

Calibration of pollutant (buildup and washoff) parameters of TSS, TP, and TN was performed following completion of calibration and validation of hydraulic parameters. The same set of hydraulic parameters applies to all subcatchments, but pollutant parameters were calibrated on a land use basis, i.e., each land use has a unique set of pollutant parameters. Pollutant parameters were calibrated based on field observation data from two USGS river gages: Walnut Creek at Webberville Road (08158600) and Walnut Creek at Dessau Road (08158200).

Field measurements of USGS observation data present the mixture of direct runoff and baseflow, so pollutant concentrations in direct runoff were further determined by Eq. 4. In Eq. 4,  $C_{dir}$  indicates the concentration of direct runoff,  $C_{mix}$  indicates the mixed concentration from USGS data,  $C_{bf}$  indicates the concentration of base flow, and BFI is the base flow index. The baseflow concentrations were calculated by averaging the concentrations from baseflow dominated events in the USGS water quality database. BFI higher than 0.95 was defined as “baseflow dominant” in this study.

$$C_{dir} = \frac{C_{mix} - C_{bf} \cdot BFI}{(1 - BFI)} \tag{4}$$

Among the 36 events, only six events are synchronized with USGS water quality measurements. All six events were used in calibration, and no validation was performed because of the low number of available data points. For each water quality constituent, two calibration runs were performed, area-based parameters and curb length-based parameters, and the one set of parameters with higher NSE is chosen. Area-based parameters were used for TSS (NSE = 0.42) and TN (NSE = 0.74), and curb length-based parameters were used for TP (NSE = 0.90) in the following analyses.

### 3.6 Derivation of Confidence Intervals of Pollutant Parameters

A large number of pollutant parameters were calibrated considering all eight land uses and four parameters for each land use, so SCEUA does not always give the same optimal solution from results of multiple runs, possibly a result of correlation between parameters. In other words, equifinality (i.e., multiple models are all acceptable to represent a system) is likely to happen. The direct effect of equifinality is the increased uncertainty in parameter estimation (Beven 2006). Some prior studies also encountered similar problems, particularly water balance models at large scales (Wilby 2005). A Monte Carlo process is often used to explore the parameter space and uncertainty.

In addition to the final optimized results given by SCEUA, simulations (prior to reaching the final optimized result) performed by SCEUA can provide useful information in uncertainty analysis (van Griensven and Meixner 2007). Therefore, useful simulations (i.e., with objective function below the upper boundary in Eq. 5

below) were gathered based on the criterion given by van Griensven and Meixner (2007):

$$c = OF \cdot \left( 1 + \frac{\chi^2_{P,CL}}{N-P} \right) \tag{5}$$

where  $c$  is the upper boundary of the objective function (the lower boundary is the optimal solution itself), OF is the objective function of the optimal solution,  $N$  is the number of observations,  $P$  is the number of parameters, and  $\chi^2_{P,CL}$  is the chi-squared statistic for  $P$  (parameter values) and CL (confidence level).

Based on the data gathered from all simulations with objective function below the criterion in Eq. 5, the result (delineated below) showed bimodal distributions for many of the parameters. Thus, a generalized lambda distribution (GLD), which has been successfully applied to fit a range of unimodal and bimodal data, was used to fit the statistical distributions (Su 2009) to derive the confidence intervals. The input value  $u$  to a GLD is the cumulative probability, and the GLD function gives the value of the variable (Karian and Dudewicz 2000). Therefore, the input value  $u$  for a GLD equation is always between 0 and 1. There are two parameterizations of the GLD equations. The first was proposed by Ramberg and Schmeiser (RS, Eq. 6), and the second was proposed by Freimer, Mudholkar, Kollia, and Lin (FMKL, Eq. 7). In Eqs. 6 and 7, the input variable is  $u$ , and  $\lambda_1, \lambda_2, \lambda_3$ , and  $\lambda_4$  are coefficients.

$$F^{-1}(u) = \lambda_1 + \frac{u^{\lambda_3} - (1-u)^{\lambda_4}}{\lambda_2} \tag{6}$$

$$F^{-1}(u) = \lambda_1 + \frac{\frac{u^{\lambda_3} - 1}{\lambda_3} - \frac{(1-u)^{\lambda_4} - 1}{\lambda_4}}{\lambda_2} \tag{7}$$

The RS GLD has a simpler form, but it requires  $\frac{\lambda_2}{\lambda_3 u^{\lambda_3-1} - \lambda_4 (1-u)^{\lambda_4-1}} \geq 0$ . The FMKL GLD only requires that  $\lambda_2$  is positive. The statistical package GLDEX for the software R was used to fit FMKL GLD.

## 4 Results

The calibrated hydraulic parameters (Table 3) show a few interesting points. First, the imperviousness area for the watershed decreased from 2001 (original value) to

**Table 3** Calibrated hydraulic parameters

Parameter	Initial value (2001)	Calibrated value (1984)	Change
Impervious percentage	Varies by subcatchment	Varies by subcatchment	- 10%
Subcatchment width	Varies by subcatchment	Varies by subcatchment	+ 246%
Manning's $n$ for impervious area	0.013	0.016	+ 23%
Manning's $n$ for pervious area	0.13	0.10	- 23%
Storage of impervious surface area	1.27 (mm)	1.27 (mm)	n/a
Storage of pervious surface area	5 (mm)	7.62 (mm)	+ 52%
Percent of impervious area with no storage	25	17.58	- 30%
Maximum infiltration rate	50 (mm/h)	79.58 (mm/h)	+ 59%
Minimum infiltration rate	0.5 (mm/h)	0.66 (mm/h)	+ 32%
Decay constant for Horton's infiltration equation	4 (1/h)	2 (1/h)	- 50%
Drying time	8 (days)	14 (days)	+ 75%
Manning's $n$ for open channels	0.03	0.031	+ 3%
Manning's $n$ for closed pipes	0.013	0.026	+ 100%

1984 (calibrated value), which matches the fact that the watershed indeed had been under development. Second, the subcatchment width increased significantly after calibration, indicating that the overland flow path is much shorter in 1984 than expected, which may indicate serious soil erosion status in early 1980s when the watershed was under development.

Based on 95% confidence level, multiple SCEUA runs were performed and data from 794 simulations, 546 simulations, and 378 simulations was gathered for TSS, TN, and TP, respectively. The relative frequency histograms of the pollutant parameters from the simulations are shown in Figs. 3, 4, and 5. Many of the parameters exhibit bimodal distributions. A Shapiro-Wilk  $W$  Test determined that none of the parameters were normally distributed with 95% confidence level.

Because the values of two parameters in Fig. 5 were smaller than the numerical precision acceptable to the intermediate data file of SCEUA, which is different from that of the final output file, they do not have distribution presented. Their confidence intervals (marked with asterisks) in Table 4 were calculated by normal distribution of the final optimized results.

## 5 Discussion

The results showed that most buildup parameters ( $C_1$  and  $C_2$ ) concentrate in narrow numerical regions.

However, many washoff parameters ( $C_3$  and  $C_4$ ) are distributed evenly. This phenomenon may indicate that pollutant buildup is controlled by factors that are spatially uniform, such as land use, temperature, or climate. On the other hand, washoff is controlled by local factors such as topography and slope. The uniform effect of climate on pollutant buildup has been studied by field experiments (Wang and Li 2009). Local factors such as topography and slope influence the runoff rate, which is the dominant factor for pollutant washoff as supported by pollutant washoff models (Rossman 2010; Soonthornnonda et al. 2008).

The USGS water quality record of Walnut Creek Watershed showed particularly high concentrations in water quality constituents. TSS from the USGS gage at the outlet of the Walnut Creek, for example, frequently reached concentrations of more than 6000 mg/L (USGS 2017a), which is much higher than anything found in literature (Hood et al. 2007; Temprano et al. 2006; Barco et al. 2004) probably due to the intense thunderstorms in summer. One would expect that this watershed has a tremendous capability to generate pollutants. Nevertheless, the results from this study showed that  $C_1$  (representing the maximum amount of pollutant per unit area or unit curb length that can provide) of many land uses is actually close to the numbers from literature (Table 1). The exceptions are  $C_1$  for bare soil, industrial, and single family land uses for TSS, bare soil, industrial, single family, and undeveloped land uses for TN, and industrial land use for TP (summarized in Table 5).

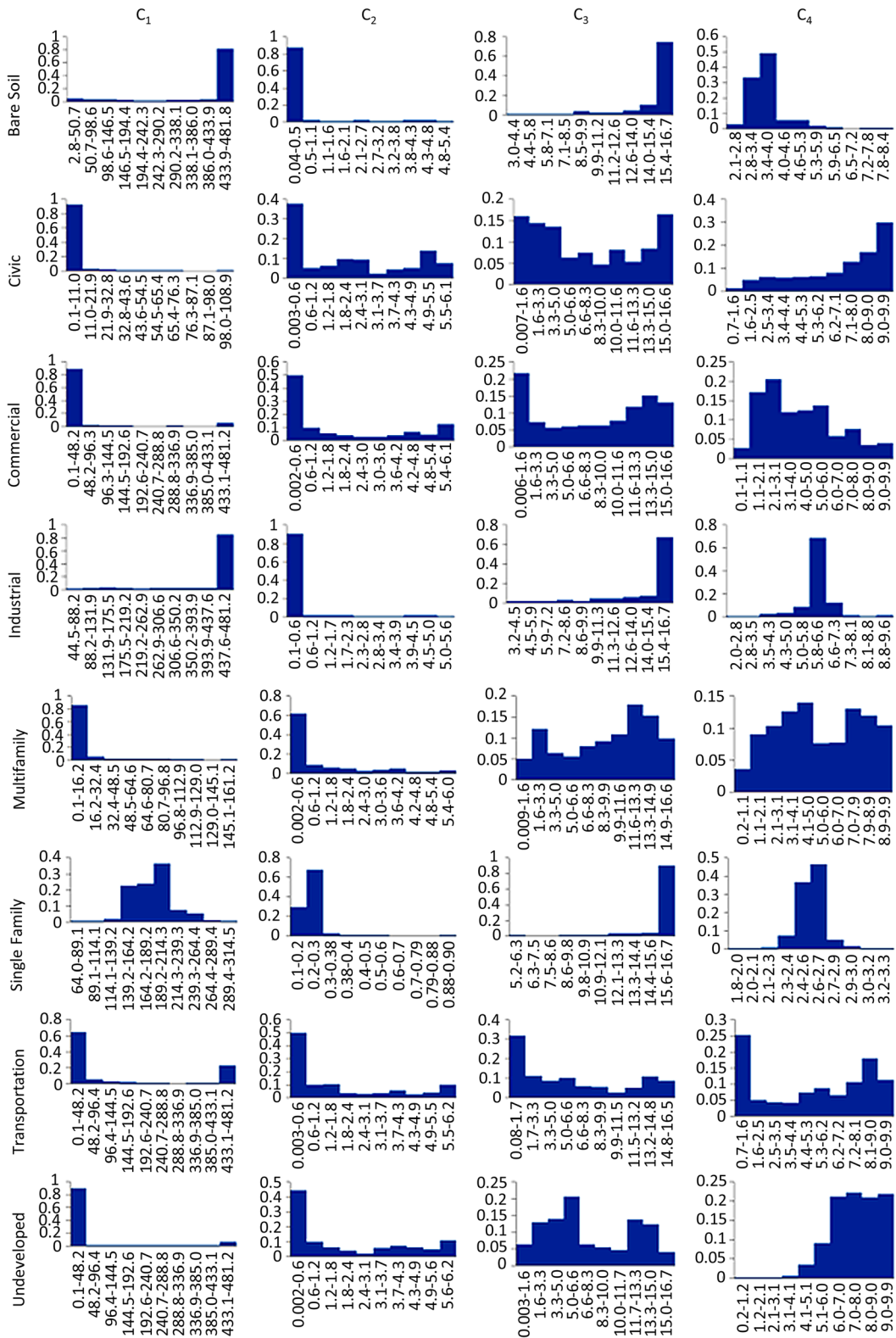


Fig. 3 Distribution of TSS pollutant parameters values

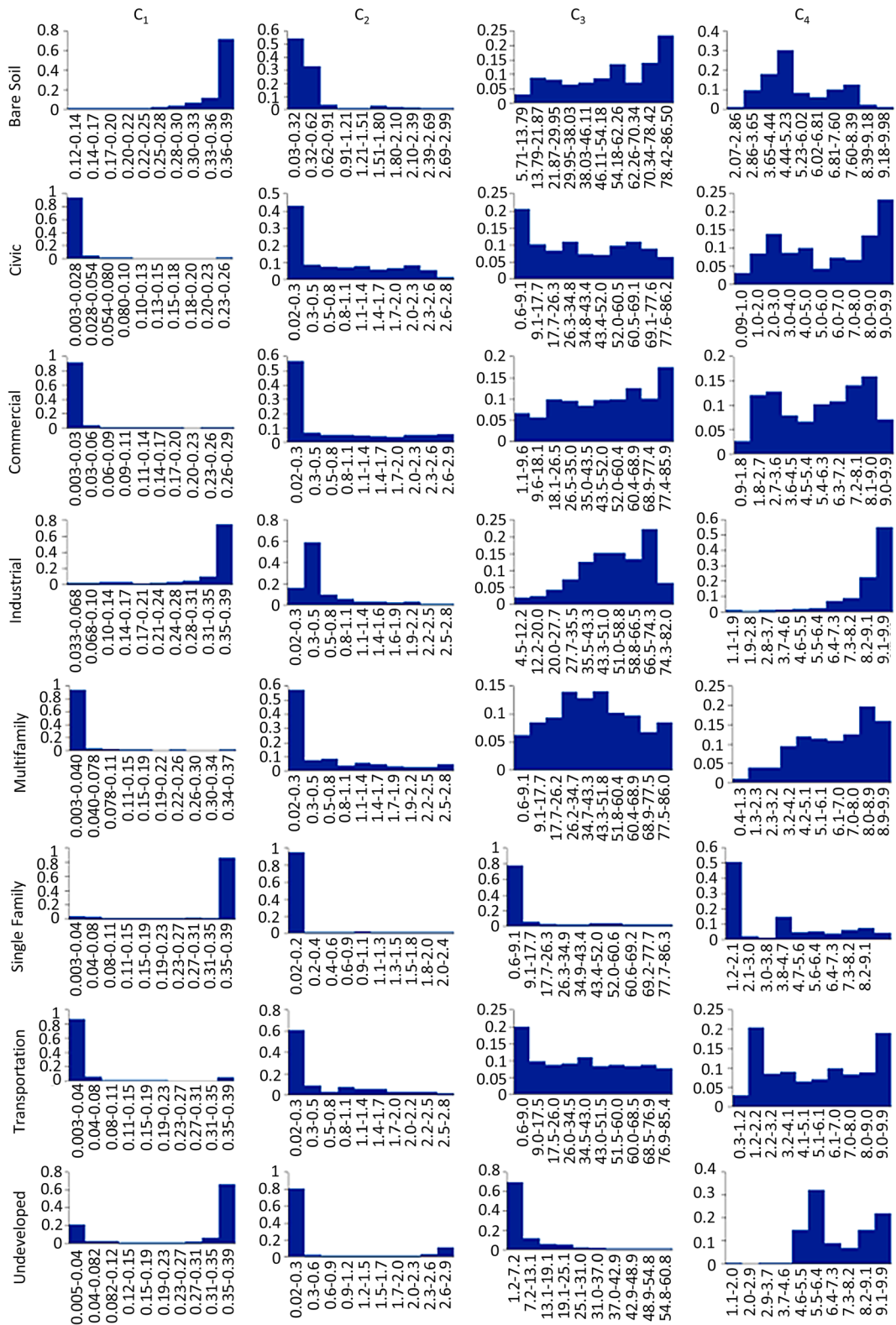


Fig. 4 Distribution of TN pollutant parameters

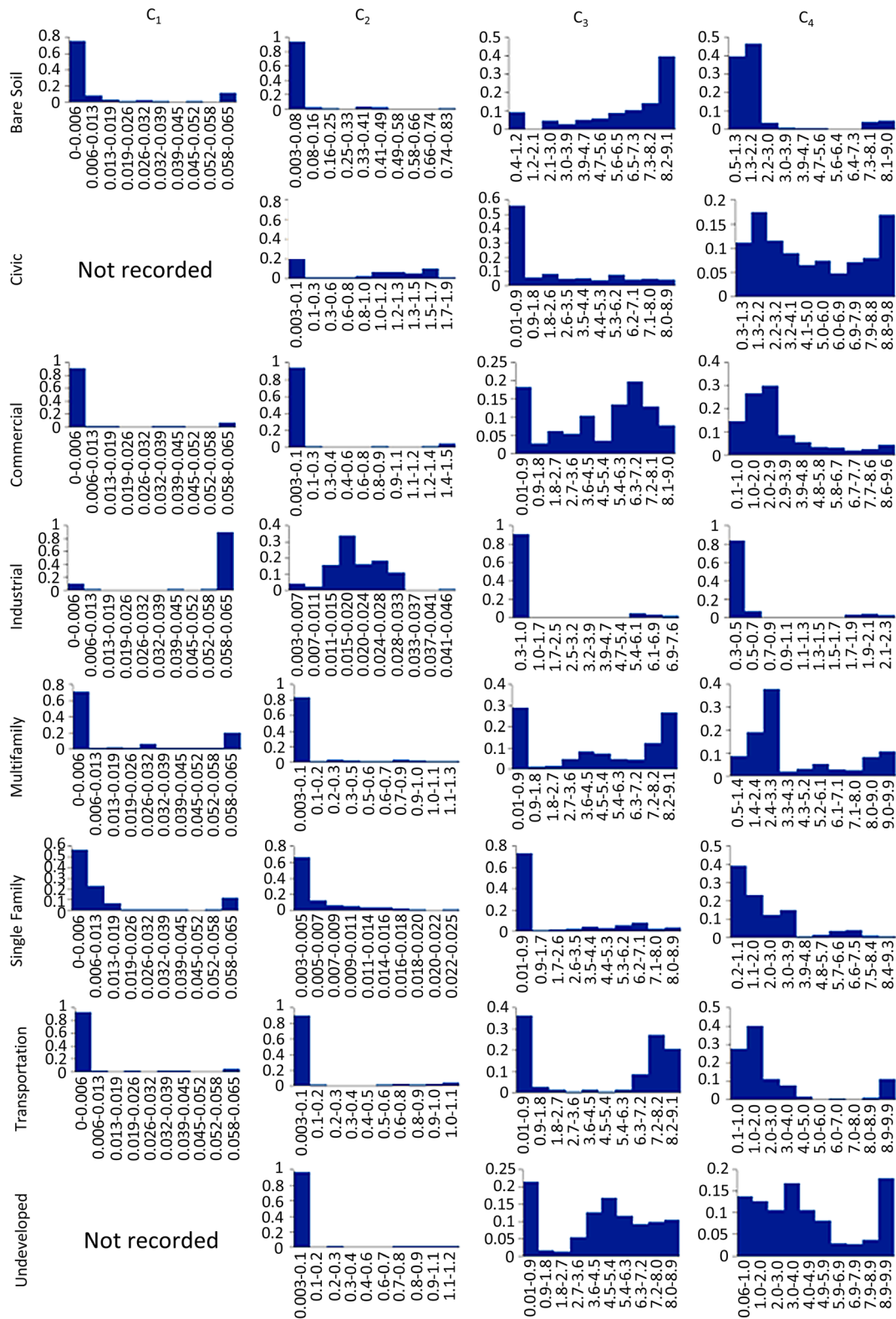


Fig. 5 Distribution of TP pollutant parameters

**Table 4** Confidence intervals of pollutant parameters for TSS, TN, and TP

Land use	Parameter	TSS (area-based): Confidence level = 95%			TN (area-based): Confidence level = 95%			TP (curb-based): Confidence level = 95%		
		Low	Mean	High	Low	Mean	High	Low	Mean	High
Bare soil	C <sub>1</sub>	337.96	429.74	465.13	0.30	0.37	0.39	2.3e-3	0.013	0.024
	C <sub>2</sub>	0.30	0.70	1.03	0.12	0.36	0.84	0.011	0.061	0.11
	C <sub>3</sub>	12.58	15.83	16.61	26.88	56.59	77.68	3.16	5.95	8.74
	C <sub>4</sub>	2.98	3.46	6.84	3.78	5.40	7.13	0.80	2.00	3.20
Civic	C <sub>1</sub>	0.03	1.42	16.49	3.5e-3	5.4e-3	0.02	1.1e-4 <sup>a</sup>	1.4e-4	1.6e-4 <sup>a</sup>
	C <sub>2</sub>	0.21	2.11	5.54	0.26	0.82	1.78	0.21	0.44	0.66
	C <sub>3</sub>	3.27	7.51	12.53	13.47	36.79	69.12	0.46	2.70	4.94
	C <sub>4</sub>	4.06	7.22	8.98	2.97	6.01	8.34	1.58	4.82	8.06
Commercial	C <sub>1</sub>	20.92	32.9	92.50	2.2e-3	0.010	0.050	2.5e-3	3.9e-3	5.2e-3
	C <sub>2</sub>	0.45	1.76	3.65	0.17	0.67	1.62	0.024	0.077	0.13
	C <sub>3</sub>	3.42	8.24	13.39	24.68	49.71	73.09	1.96	4.68	7.40
	C <sub>4</sub>	1.87	4.11	7.42	3.05	5.85	8.13	0.95	3.41	5.87
Industrial	C <sub>1</sub>	380.72	448.91	470.46	0.26	0.36	0.38	0.049	0.058	0.067
	C <sub>2</sub>	0.32	0.59	1.05	0.23	0.56	1.28	0.011	0.019	0.027
	C <sub>3</sub>	11.24	15.18	16.25	25.69	54.21	68.86	0.77	1.01	1.25
	C <sub>4</sub>	4.54	6.28	7.48	5.32	8.89	9.89	0.51	0.67	0.83
Multifamily	C <sub>1</sub>	1.00	6.84	32.35	3.8e-3	0.010	0.045	6e-3	0.021	0.035
	C <sub>2</sub>	0.09	0.88	2.58	0.12	0.60	1.53	0.028	0.20	0.37
	C <sub>3</sub>	4.15	9.59	14.12	13.24	43.02	68.07	1.99	2.00	7.60
	C <sub>4</sub>	2.31	5.49	8.05	3.59	6.61	8.58	1.76	4.16	6.55
Single family	C <sub>1</sub>	159.55	181.40	329.00	0.30	0.36	0.38	3.9e-3	0.031	0.027
	C <sub>2</sub>	0.20	0.22	0.31	0.034	0.061	0.17	3.4e-3	7.2e-3	0.011
	C <sub>3</sub>	15.32	16.49	16.73	2.46	8.73	27.84	0.76	1.83	2.90
	C <sub>4</sub>	2.51	2.62	2.85	2.00	3.66	6.17	0.60	2.70	4.80
Transportation	C <sub>1</sub>	89.28	117.29	232.61	0.016	0.030	0.087	1.6e-3	3e-3	4.3e-3
	C <sub>2</sub>	0.29	1.55	3.77	0.21	0.51	1.35	0.067	0.12	0.18
	C <sub>3</sub>	1.64	5.46	13.39	11.38	37.01	66.56	3.05	4.73	6.40
	C <sub>4</sub>	1.76	5.52	7.96	2.29	5.51	8.91	1.38	2.92	4.46
Undeveloped	C <sub>1</sub>	14.39	37.54	83.98	0.22	0.30	0.34	1.1e-4 <sup>a</sup>	1.3e-4	1.4e-4 <sup>a</sup>
	C <sub>2</sub>	0.58	2.09	4.55	0.19	0.47	0.79	0.018	0.036	0.053
	C <sub>3</sub>	3.54	7.68	11.43	4.25	7.94	19.48	2.37	4.78	7.18
	C <sub>4</sub>	5.37	7.78	9.16	5.40	7.18	8.57	1.38	4.77	8.15

<sup>a</sup> Calculated by normal distribution from final optimized values

These land uses in Table 5 are potentially the major sources of non-point pollutions. The result of undeveloped land use providing a large quantity of TN but not TSS may indicate the existence of manure sources from free-ranging Texan cattle. As for TP, pollutant generation capability for commercial and industrial land uses should be similar, according to Chow et al. (2013). The disparity in pollutant generating capability for

commercial and industrial land uses, and the high TP generating capability for industrial land use, is worth investigating.

After further examination, this phenomenon can be contributed to the fact that many industrial sites were newly built or under construction in 1984 (particularly the large industrial park in the western part of the watershed). Therefore, their TSS generation characteristics

**Table 5** Land uses with high capacity to provide pollutants for non-point pollution

	TSS	TN	TP
Bare soil	x	x	
Industrial	x	x	x
Single family	x	x	
Undeveloped		x	

should be close to bare soil. The use of fertilizer to facilitate plant growth in newly constructed sites may explain why industrial land use has high TN and TP exports. Therefore, it may be appropriate to ignore parameters for industrial land use, and instead use the parameters from commercial land use for industrial areas.

The parameter  $C_2$  governs the speed of pollutant buildup. Among all water quality constituents, the values of  $C_2$  for most land uses stay in the same numerical range. For TSS,  $C_2$  stays in the range of approximately 0–0.6. For TN,  $C_2$  stays in the range of approximately 0–0.3. For TP,  $C_2$  stays in the range of approximately 0–0.1 except for the land uses of industrial and single family. This indicates that pollutant buildup is mainly controlled by factors that are spatially distributed, such as land use, temperature, or climate.

The parameters  $C_3$  and  $C_4$  both control the washoff rate of water quality constituents, with  $C_3$  the coefficient and  $C_4$  the exponent of the equation. Numerical distributions of these parameters are more diverse indicating the influence of local factors that control runoff rates.

For  $C_4$ , it is interesting to compare the washoff equation (Eq. 2) with the equation of shear stress (Eq. 8) along a channel provided by:

$$\tau = \gamma R s \quad (8)$$

In Eq. 8,  $\tau$  is the shear stress at the bottom of the channel (N/m),  $\gamma$  is the specific weight of water (9.81 kN/m<sup>3</sup>),  $R$  is the hydraulic radius (m<sup>2</sup>/m), and  $s$  is slope (m/m). For overland flow where width is much larger than depth, the hydraulic radius  $R$  is close to the depth of runoff. Given the same shear stress, pollutant washoff can be assumed to be proportional to the amount of available pollutant buildup on the surface. Therefore, Eqs. 8 to 2 are linked as shown in Eq. 9.

$$\tau = \gamma R s \propto (\gamma s) \cdot \text{Runoff} \propto C_3 \cdot \text{Runoff}^{C_4} \quad (9)$$

The unit of runoff is depth/h. Equation 9 implies that the value of  $C_4$  should be close to 1 under ideal

conditions. This agrees with values found in the literature (Wicke et al. 2012; Temprano et al. 2006). However, this study found that  $C_4$  is not close to 1 for many land uses. The use of the conventional value of 1 for  $C_4$  can result in large errors.

## 6 Conclusion

The methodology depicted by this study has shown to derive reasonable results for multiple land uses from limited data input. For buildup parameters ( $C_1$  and  $C_2$ ), they are governed by mechanisms uniform in space, such as land use, temperature, or climate, so the derived parameters are also distributed in narrow numerical ranges. On the other hand, washoff parameters ( $C_3$  and  $C_4$ ), which are controlled by local factors such as topography and slope, have derived parameters scattered more uniformly.

Also, the semiarid urban watershed showed higher sediment generation capability (USGS 2017a) compared to that from other literature studies in Table 1, which were performed in cities of humid climate. The derived parameters from this study can provide a baseline for modeling pollutant generation and delivery in semiarid urban watersheds worldwide.

This study also showed that some of the conventional values for pollutant parameters might not be accurate in the field. Using them in modeling can lead to large errors.

Nevertheless, this study still leaves space for improvements. Many new industrial sites under construction were identified as industrial, while their pollutant generation and delivery characteristic are actually close to bare soil, which greatly distorted the derived parameters for industrial land use. Therefore, parameters of commercial land use should be used to replace those of industrial land use, since the two land uses showed similar pollutant loadings in field observations (Chow et al. 2013). For future studies adopting the approach of this study, urban watersheds under rapid transition (like the Walnut Creek watershed used in this study) should be avoided because newly developed area may exhibit different pollutant buildup and/or washoff characteristics.

**Acknowledgements** The support of data from city of Austin, TX, was highly appreciated.

## References

- Barco O.J., Ciaponi C., & Papiri S. (2004). Pollution in storm water runoff—two cases: an urban catchment and a highway toll gate area. *Novatech*, 1–8.
- Beven, K. (2006). A manifesto for the equifinality thesis. *Journal of Hydrology*, 320, 18–36.
- Chow, M. F., Yusop, Z., & Toriman, M. E. (2012). Modelling runoff quantity and quality in tropical urban catchments using storm water management model. *International journal of Environmental Science and Technology*, 9, 737–748.
- Chow, M. F., Yusop, Z., & Shirazi, S. M. (2013). Storm runoff quality and pollutant loading from commercial, residential, and industrial catchments in the tropic. *Environmental Monitoring and Assessment*, 185, 8321–8331.
- City of Austin. (2017). GIS Data. City of Austin. <http://austintexas.gov/department/gis-and-maps/gis-data>. Accessed 30 November 2017.
- Doherty, J. (2010). *PEST: Model-independent Parameter Estimation User Manual* (5th ed.). Queensland: Watermark Numerical Computing.
- Duan, Q. Y., Gupta, V. K., & Sorooshian, S. (1993). Shuffled complex evolution approach for effective and efficient global minimization. *Journal of Optimization Theory and Applications*, 76(3), 501–521.
- Fischer, A., Rouault, P., Kroll, S., Assel, J. V., & Pawlowsky-Reusing, E. (2009). Possibilities of sewer model simplifications. *Urban Water Journal*, 6(6), 457–470.
- Hernandez, M., Miller, S. N., Goodrich, D. C., Goff, B. F., Kepner, W. G., Edmonds, C. M., & Jones, K. B. (2000). Modeling runoff response to land cover and rainfall spatial variability in semi-arid watersheds. *Environmental Monitoring and Assessment*, 64, 285–298.
- Hood, M., Reihan, A., & Loigu, E. (2007). Modeling urban stormwater runoff pollution in Tallinn, Estonia. *Proceedings of International Symposium on New Directions in Urban Water Management*. Paris, France: United Nations Educational, Scientific, and Cultural Organizations.
- Hossain, I., Imteaz, M., Gate-Trinidad, S., & Shanableh, A. (2010). Development of a catchment water quality model for continuous simulations of pollutants build-up and wash-off. *International Journal of Civil and Environ. Eng.*, 2(4), 210–217.
- Hossain, I., Imteaz, M. A., & Hossain, M. I. (2012). Application of a catchment water quality model for an East-Australian catchment. *International Journal of Global Environmental Issues*, 12, 242–255.
- Huber, W. C., & Dickinson, R. E. (1988). *Storm Water Management Model, Version 4: User's Manual*. Athens, GA: U.S. Environmental Protection Agency.
- Ines, A. V. M., & Droogers, P. (2002). Inverse modelling in estimating soil hydraulic functions: a genetic algorithm approach. *Hydrology and Earth System Sciences Discussions, European Geosciences Union*, 6(1), 49–66.
- Karian, Z. A., & Dudewicz, E. J. (2000). *Fitting statistical distributions: the generalized lambda distribution and generalized bootstrap methods*. Boca Raton, FL: CRC Press.
- Leitao, J. P., Simoes, N. E., Maksimovic, C., Ferreira, F., Prodanovic, D., Matos, J. S., & Sa Marques, A. (2010). Real-time forecasting urban drainage models: full or simplified networks? *Water Sci. and Tech.*, 62(9), 2106–2114.
- Lim, K. J., Engel, B. A., Tang, Z., Choi, J., Kim, K.-S., Muthukrishnan, S., & Tripathy, D. (2005). Automated web GIS based hydrograph analysis tool, WHAT. *Journal of the American Water Resources Association*, 41(6), 1407–1416.
- Multi-Resolution Land Characteristics Consortium (2017). National Land Cover Database (NLCD). U.S. Geological Survey. <http://www.mrlc.gov/index.php>. Accessed 30 Nov 2017.
- National Climatic Data Center (2017). National Climatic Data Center. National Climatic Data Center. <http://www.ncdc.noaa.gov/about-ncdc>. Accessed 30 November 2017.
- Natural Resources Conservation Services (2017). Web Soil Survey. NRCS, Office of the Chief. <http://websoilsurvey.sc.egov.usda.gov/App/HomePage.htm>. Accessed 30 Nov 2017.
- Park, M.-H., Swamikannu, X., & Stenstrom, M. K. (2009). Accuracy and precision of the volume concentration method for urban stormwater modeling. *Water Research*, 43, 2773–2786.
- Rossmann, L. A. (2010). *Storm Water Management Model User's Manual, Version 5.0*. Cincinnati, OH: National Risk Management Research Laboratory.
- Ruelland, D., Ardoin-Bardin, S., Billen, G., & Servat, E. (2008). Sensitivity of a lumped and semi-distributed hydrological model to several methods of rainfall interpolation on a large basin in West Africa. *Journal of Hydrology*, 361, 96–117.
- Scanlon, B. R., Keese, K. E., Flint, A. L., Flint, L. E., Gaye, C. B., Edmunds, W. M., & Simmers, I. (2006). Global synthesis of groundwater recharge in semiarid and arid regions. *Hydrological Processes*, 20, 3335–3370.
- Soonthornnonda, P., Christensen, E. R., Liu, Y., & Li, J. (2008). A washoff model for stormwater pollutants. *The Science of the Total Environment*, 402, 248–256.
- Su, S. (2009). Confidence intervals for quantiles using generalized lambda distributions. *Computational Statistics and Data Analysis*, 53, 3324–3333.
- Temprano, J., Arango, O., Cagiao, J., Suarez, J., & Tejero, I. (2006). Stormwater quality calibration by SWMM: a case study in Northern Spain. *Water SA*, 32(1), 55–63.
- Tsihrintzis, V. A., & Hamid, R. (1997). Modeling and management of urban stormwater runoff quality: a review. *Water Resources Management*, 11(2), 136–164.
- United States Environmental Protection Agency (1983). *Results of the nationwide urban runoff program*. WH-544. Water Planning Division, U.S. EPA. [http://www.epa.gov/npdes/pubs/sw\\_nurp\\_vol\\_1\\_finalreport.pdf](http://www.epa.gov/npdes/pubs/sw_nurp_vol_1_finalreport.pdf). Accessed 30 Nov 2017.
- United States Geological Survey (2017a). USGS water data for the nation. United States Geological Survey Headquarters. <http://waterdata.usgs.gov/nwis/>. Accessed 30 Nov 2017.
- United States Geological Survey (2017b). The national map viewer and download platform. United States Geological Survey Headquarters. <http://viewer.nationalmap.gov/viewer/>. Accessed 30 Nov 2017.
- Urbanas, B., & Stahre, P. (1993). *Stormwater best management practices and detention for water quality, drainage, and CSO management*. Englewood Cliffs, NJ: PTR Prentice-Hall.

- Van Griensven, A., & Meixner, T. (2007). A global and efficient multi-objective auto-calibration and uncertainty estimation method for water quality catchment models. *Journal of Hydroinformatics*, *9*(4), 277–291.
- Wang, B., & Li, T. (2009). Buildup characteristics of roof pollutants in the Shanghai urban area, China. *Journal of Zhejiang University. Science. A*, *10*(9), 1374–1382.
- Wicke, D., Cochrane, T. A., & O’Sullivan, A. (2012). Build-up dynamics of heavy metals deposited on impermeable urban surfaces. *Journal of Environmental Management*, *113*, 347–354.
- Wilby, R. L. (2005). Uncertainty in water resource model parameters used for climate change impact assessment. *Hydrological Processes*, *19*, 3201–3219.